NASA Technical Memorandum 100569

MINIMUM WEIGHT DESIGN OF ROTORCRAFT BLADES WITH MULTIPLE FREQUENCY AND STRESS CONSTRAINTS

Aditi Chattopadhyay and
Joanne L. Walsh

March 1988

National Aeronautics and
Space Administration

Langley Research Center
Hampton, Virginia 23665

Minimum Weight Design of Rotorcraft Blades with Multiple Frequency and Stress Constraints

by

Aditi Chattopadhyay
Analytical Services & Materials, Inc.
Hampton, Virginia 23666
and

Joanne L. Walsh
NASA Langley Research Center
Hampton, Virginia 23665

Abstract

The minimum weight design of helicopter rotor blades with constraints on multiple coupled flap-lag natural frequencies has been studied in this paper. A constraint has also been imposed on the minimum value of the autorotational inertia of the blade to ensure sufficient rotary inertia to autorotate in case of an engine failure. A stress constraint has been used to guard against structural failure due to blade centrifugal forces. Design variables include blade taper ratio, dimensions of the box beam located inside the airfoil and magnitudes of the nonstructural weights. The program CAMRAD has been used for the blade modal analysis and the program CONMIN has been used for the optimization. In addition, a linear approximation involving Taylor series expansion has been used to reduce the analysis effort. The procedure contains a sensitivity analysis which consists of analytical derivatives of the objective function, the autorotational inertia constraint and the stress constraints. A central finite difference scheme has been used for the derivatives of the frequency constraints. Optimum designs have been obtained for both rectangular and tapered blades. Using the method developed in this paper, it is possible to design a rotor blade with reduced weight, when compared to a baseline blade, while satisfying all the imposed design requirements. The paper also discusses the effect of adding constraints on higher frequencies and stresses on the optimum blade weight and the distributions of mass and stiffness in the optimum designs.

Nomenclature

b	box beam width
c	chord
f_1, f_3, f_4	first three lead-lag dominated frequencies (elastic modes)
f_2, f_5	first two flapping dominated frequencies (elastic modes)
g	constraint function
h	box beam height
$h(z)$	box beam height variation along blade span
n	number of blades
r_j	distance from the root to the center of the j^{th} segment
t_1, t_2, t_3	box beam wall thicknesses
x, y, z	reference axes
A	box beam cross sectional area
AI	autorotational inertia
E	Young's modulus
F	objective function
FS	factor of safety
GJ	torsional stiffness
I_x, I_y	total principal area moments of inertia about reference axes
L_j	length of j^{th} segment
M_j	total mass of j^{th} segment
N	total number of blade segments
NDV	number of design variables
R	blade radius
W	total blade weight
$W(\phi)$	blade weight as a function of design variable ϕ
W_b	box beam weight
W_o	nonstructural blade weight (weight of skin, honeycomb, etc. along with tuning/lumped weights)
α	prescribed autorotational inertia
$\Delta\phi$	design variable increment
λ_h	taper ratio in z direction
ϕ_i	i^{th} design variable
ρ_j	mass density of the j^{th} segment
σ_j	stress in j^{th} segment
σ_{max}	maximum allowable stress
Ω	blade RPM

Subscripts and Superscripts

r	root value
t	tip value
L	lower bound
U	upper bound
$\hat{}$	approximate value

Introduction

Computer-based mathematical programming methods for optimum design of structures have been under rapid development during the last two decades. Using mathematical processes, engineering design synthesis problems can be posed as sequences of analysis problems combining engineering models with minimization techniques. An extensive amount of work has been done in developing such design optimization procedures over the past few years to bring the state of the art to a high level[1-5]. These methods can now be applied to optimum design of practical structures such as aircraft[1,2,5] and helicopters[3-5]. The present paper focuses on helicopter rotor blade design.

The helicopter rotor blade design process requires a merging of several disciplines, including dynamics, aerodynamics, structures, and acoustics. Two of the major criteria in rotor blade design have been low weight and low vibration. For a helicopter in forward flight, the nonuniform flow passing through the rotor causes oscillating airloads on the rotor blades. These loads in turn are translated into vibratory shear forces and bending moments at the hub. One important design technique is to separate the natural frequencies of the blade from the harmonics of the airloads to avoid resonance. Failure to consider frequency placement in the predesign stage of the design process could cause a significant increase in the final blade weight since it generally involves postdesign addition of nonstructural masses. To avoid such weight penalties it is desirable in the design and fabrication of the blade to appropriately place the natural frequencies at an early stage in the design process. This can be done by a proper tailoring of the blade mass and/or stiffness distribution. This tailoring is not an easy task because of the complicated vibration modes of the blade due to the presence of several coupling effects[6]. One such coupling is between flap, lag, and torsional motions through the pitch angle blade twist and offset between the elastic and inertia axes. The inclusion of these coupling effects makes the design process highly complex. In the past, the conventional design process was controlled mainly by the designer's experience and the use of trial and error methods.

Today, one of the more promising approaches to the helicopter rotor design process is the application of optimization techniques. A considerable amount of work has been aimed at optimum designs of vibrating structures. For example, minimum weight designs with constraints on natural frequencies have been addressed in Refs. 7-9 and the dual problem of maximizing the frequencies with a constraint on the total weight has been addressed in Ref. 10. Frequencies of coupled bending-torsion modes caused by an offset between the elastic and inertia axes have been addressed in Refs. 9 and 10. Recently there have been a number of applications of optimization techniques to rotor blade design[5,6,11-19]. Some of this work has been devoted to reducing vibration by controlling the vertical hub shears and moments[12-17]. In Ref. 13 Taylor described the use of modal shaping. The objective of his work is to reduce vibration levels by modifying 'modal shaping parameters' which are functions of blade mass distributions and mode shapes. These modal shaping parameters have been sometimes interpreted as 'ad hoc' optimality criteria[15,17]. In Ref. 14 Bennett described a method for reducing the vertical shear transferred from the rotor blade to the mast by combining conventional helicopter engineering analysis with a nonlinear programming algorithm. Friedmann[15] considered the problem of minimizing hub shears or hub vibratory rolling moments subject to aeroelastic and frequency constraints. An early attempt at optimum blade design for proper placement of natural frequencies with a constraint on autorotational inertia was due to Peters[16] where he started with a baseline blade design and attempted to refine the design by trying to find a mass and stiffness distribution to give the desired frequencies. Reference 17 addressed the optimum design for a typical soft in-plane hingeless rotor configuration for minimum weight using optimality criteria approach. The results in Ref. 17 indicate that application of optimization techniques leads to benefits in rotor blade design not only through substantial weight reduction but also a considerable reduction in the vibratory hub shears and moments at the blade root. In Ref. 18, Peters addressed a problem of the optimum design of a rectangular blade for proper placement of frequencies. However, he did not use the blade weight as the objective function due to a difficulty in finding a feasible initial design. Rather, he started his design with an objective function involving measures of the closeness of frequencies to desirable frequencies.

Currently at the NASA Langley Research Center, there is an effort to integrate several technical disciplines in rotorcraft design. The present work is part of this effort and deals with the dynamics aspect of design. The problem addressed in this paper is an extension of the problem addressed by the authors in Ref. 19 where constraints were imposed on the first lead-lag dominated mode and the first flapping dominated mode along with a rotary inertia constraint to assure that the blade could autorotate. The structural safety of the design was included as a first approximation by imposing lower bounds on the structural design variables. However, the danger of the higher frequencies falling in the critical ranges and causing resonance remained. The current work involves minimum weight designs of helicopter rotor blades subject to the following constraints: a) upper and lower bounds ('windows') on multiple adjacent natural frequencies, b) minimum prescribed value on the blade autorotational inertia, and c) upper limit on the blade centrifugal stress. In Ref. 18 Peters addressed the necessity of using a stress constraint in frequency placement optimization but did not include it in the optimization formulation. The expression for the stress presented here differs from that of Ref. 18 and is a more conservative estimate. An existing adequate blade which will be referred to as the 'reference blade' has been selected. In rotor blade design it is essential for natural frequencies to be separated from values which are certain

integer multiples of the rotor speed to avoid resonance. These critical values are referred to as 'n per rev' where n denotes the total number of blades. A modal analysis of the reference blade showed that the frequencies of interest were away from the n per rev values. Hence, it was decided to define the frequency constraints to force the frequencies to be close to those of the reference blade. This is done by optimally tailoring the blade stiffness and mass distributions by the procedure developed in this paper. The purpose of this paper is to describe the formulation and implementation of the optimization procedure, present results from the procedure and assess the effects of additional frequency and stress constraints on the optimum designs.

Optimization Problem Formulation

The purpose of the optimization procedure is to reduce the weight of a blade while constraining the natural frequencies to be within the 'windows' of the reference blade frequencies. The concept of 'windows' has been used since the nonlinear programming method used in this work cannot handle equality constraints. These windows are on the frequencies of the first three lead-lag dominated modes and the first two flapping dominated modes (elastic modes only). A prescribed lower limit on the blade autorotational inertia and an upper bound on the blade centrifugal stress have also been used. Side constraints have been imposed on the design variables to avoid impractical solutions. The design variables include box beam dimensions, taper ratio and magnitudes of the nonstructural weights located inside the box beam. The optimization process begins with an arbitrary set of design variable values.

The blade weight, W, has two components as follows:

$$W = W_b + W_o \tag{1}$$

where W_b denotes the box beam weight and W_o represents the nonstructural weight of the blade which includes the weight of the skin, honeycomb, etc., along with the weight of the tuning/lumped masses added to the blade. The blade is discretized into finite segments and the blade weight in discretized form is given below:

$$W = \sum_{j=1}^{N} \rho_j A_j L_j + \sum_{j=1}^{N} W_{o_j} \tag{2}$$

where N denotes the total number of segments and ρ_j, A_j, L_j and W_{o_j} denote the density, the cross sectional area, the length and the nonstructural weight of the j^{th} segment, respectively.

The autorotational inertia (AI) of the blade is calculated as follows

$$AI = \sum_{j=1}^{N} W_j r_j^2 \tag{3}$$

where W_j is the total weight and r_j is the distance from the root to the center of the j^{th} segment. The expression for the blade stress is

$$\sigma_i = \sum_{j=i}^{N} M_j \Omega^2 r_j / A_i \tag{4}$$

where σ_i is the stress due to centrifugal forces and A_i is the cross sectional area of the i^{th} segment, M_j is the total mass of the j^{th} segment and Ω is the blade RPM. The frequencies associated with the first five elastic modes of coupled vibration are denoted by f_1, f_2, f_3, f_4 and f_5, (includes three lead-lag and two flapping).

The optimization problem can now be mathematically posed as follows:

$$\text{minimize } W(\phi)$$

where the weight W is given by equation (2) and ϕ denotes the vector of design variables, subject to the normalized constraints

$$g_k(\phi) = (f_k/f_{k_U}) - 1 \le 0 \qquad k=1,2,..,5 \tag{5}$$

$$g_{k+5}(\phi) = 1 - (f_k/f_{k_L}) \le 0 \qquad k=1,2,..,5 \tag{6}$$

$$g_{11}(\phi) = 1 - (AI/\alpha) \le 0 \tag{7}$$

$$g_{11+k}(\phi) = 1 - \sigma_{max}/(\sigma_k \cdot FS) \le 0 \quad k=1,2,..,N \tag{8}$$

and side constraints

$$\phi_{i_L} \le \phi_i \le \phi_{i_U} \tag{9}$$

In equations (5) and (6), f_{k_U} and f_{k_L}, denote the upper and lower bound on the k^{th} frequency f_k. In equation (7) α represents the minimum prescribed autorotational inertia value. In equation (8) σ_k is the stress in the k^{th} segment given by equation (4), σ_{max} is the maximum allowable stress in the blade and FS is a factor of safety. In equation (9) ϕ_i denotes the i^{th} design variable and ϕ_{i_U} and ϕ_{i_L} represent the associated upper and lower bounds, respectively. By convention a constraint $g(\phi)$ is satisfied when $g(\phi) \le 0$.

Analysis

The modal analysis portion of the program CAMRAD[20] which uses a modified Galerkin

approach[21] has been used. According to Ref. 22, this approach is the preferred method for computing mode shapes and frequencies of structures having large radial variations in bending stiffness. Analytical expressions have been obtained for the derivatives of the objective function, the autorotational inertia constraint and the stress constraints. A central difference scheme has been used for the derivative of the frequency constraints (initial attempts using a forward difference scheme gave highly inaccurate derivatives).

Optimization Implementation

The basic algorithm used is a combination of the general-purpose optimization program CONMIN[23] and piecewise linear approximations for computing the objective function and constraints. Since the optimization process requires many evaluations of the objective function and constraints before an optimum design is obtained, the process can be very expensive if full analyses are made for each function evaluation. However, as Miura[3] pointed out, the optimization process primarily uses analysis results to move in the direction of the optimum design; therefore, a full analysis needs to be made only occasionally during the design process and always at the end to check the final design. Thus, various approximation techniques can be used during the optimization to reduce costs. In the present work, the objective function and constraints are approximated using a piecewise linear analysis that consists of linear Taylor series expansions for the objective function and the constraints based on the design variable values from CONMIN and the sensitivity information from the full analysis. Specifically, if the objective function F, the constraint g, and their respective derivatives are calculated for the design variable ϕ_k using an exact analysis, their values for an increment in the design variable $\Delta\phi_k$ are as follows:

$$\hat{F} = F + \sum_{k=1}^{NDV} (\partial F/\partial \phi_k)\Delta\phi_k \qquad (10)$$

and

$$\hat{g} = g + \sum_{k=1}^{NDV} (\partial g/\partial \phi_k)\Delta\phi_k \qquad (11)$$

where the quantities denoted (^) represent approximate values and NDV denotes the number of design variables. The assumption of linearity is valid over small increments in the design variable values and does not introduce large errors if the increments are small. Since the objective function and the constraints are all linearized, the optimization problem reduces to essentially a sequential linear programming problem.

A flow chart describing the optimization procedure is shown in Fig. 1. The iteration scheme is stopped when the objective function converges. For the convergence of the objective function, a change within a convergence tolerance of 0.5×10^{-5} over three consecutive cycles has been allowed.

Test Problem

The reference blade (Refs. 18-19) shown in Fig. 2 is articulated and has a rigid hub. The blade has a rectangular planform, a pretwist and a root spring which allows torsional motion. The box beam with unequal vertical wall thicknesses is located inside the airfoil. As in Ref. 19, it is assumed that the box beam contributes to the blade stiffness and the contributions of the skin, honeycomb, etc. to the blade stiffness are neglected. The details for calculating the box beam section properties can be found in the Appendix of Ref. 19. The properties of the box beam located inside the airfoil (Fig. 2) are as follows:

$h=0.117$ ft
$b=0.463$ ft
$\rho=8.645$ slugs/ft^3
$E=2.304 \times 10^9$ lb/ft^2

An allowable stress $\sigma_{max}=1.93\times10^7$lb/ft^2 and a factor of safety FS=3 have been used in the analysis. The blade has been discretized into ten segments and details of the blade segment data are presented in Table 1. The entry 'min. nonstructural segment weight' in Table 1 represents the weight of the skin, honeycomb, etc. of a segment and 'total nonstructural segment weight' represents the weight of the skin, honeycomb, etc. along with the lumped/tuning weight of that segment. The rotor preassigned parameters (the parameters that remain fixed during the optimization process) are presented in Table 2.

The frequencies of interest of the reference blade are presented in Table 3. The first three lead-lag dominated and the first two flapping dominated modes are away from the critical frequencies (e.g., 3, 4, 5 and 8 per rev) and need not be improved further. Therefore, the frequency windows for the optimum blade are set to be within ±1 percent of these values (Table 3).

Blades with both rectangular and tapered planforms have been considered. In case of the rectangular blade, the box beam is uniform along the blade span. For the tapered blade it is assumed, as in Ref. 19, that the box beam is tapered (Fig. 3a) and the additional design variables are the box beam height at the root, h_r, and the taper ratio, λ_h, which is defined as the ratio of the box beam height at the root to the corresponding value at the tip (Fig. 3a). As in Ref. 19, a linear variation of the box beam height, h, in the spanwise direction (z direction) has been assumed (Fig. 3b).

Results and Discussion

This section of the paper presents results obtained by applying the optimization procedure, described previously, to the optimum design of both rectangular and tapered rotor blades. First, optimum designs are described and compared with the reference

blade (Refs. 18 and 19). Second, results of a study assessing the effects of including constraints on higher frequencies are described. Finally, the effects of stress constraints have been investigated by comparing the results obtained with stress constraints to those without stress constraints. A summary of the cases studied is given in Table 4. Results of these studies are presented in Tables 5 and 6 for the rectangular blade (30 and 40 design variables) and in Table 7 for the tapered blade (42 design variables). In each table, column 1 represents the reference blade data; column 2 gives the corresponding information for the optimum design with constraints on the five frequencies, autorotational inertia and stress (case a, Table 4); column 3 gives results for the optimum design with constraints on the five frequencies and autorotational inertia only (no stress constraints, case b, Table 4) and column 4 presents the results (Ref. 19) for the optimum design with constraints on the first two frequencies (elastic modes only) and autorotational inertia (case c, Table 4). In all cases convergence typically has been achieved in 8-10 cycles.

The tables indicate that with the constraints on the five frequencies, the autorotational inertia and the blade stresses, the optimum rectangular blade is 2.67 to 4.74 percent lighter than the reference blade and the optimum tapered blade is 6.21 percent lighter than the reference blade. The first lead-lag frequency (f_1) is at its prescribed upper bound after optimization and the autorotational inertia constraint is active (i.e. exactly satisfied) in all cases. The associated design variable distributions are presented in Figs. 4-6. Fig. 4a presents the optimum versus the reference blade box beam horizontal wall thickness (t_1) distributions along the blade span for the rectangular blade and Fig. 4b presents the same for the tapered blade. In both cases, the optimum blade has a larger value of t_1 than the reference blade at the blade tip and in case of the tapered blade the value of t_1 at the blade root is much smaller than the value for the reference blade. Figs. 5a and 5b present the optimum versus the reference blade box beam vertical wall thickness (t_2) distributions along the blade span for the rectangular and the tapered blade, respectively. The optimization process does not produce significant changes in the t_2 distribution for the rectangular blade (Fig. 5a). The changes are more significant for the tapered blade (Fig. 5b) where there are larger values of t_2 towards the blade tip. The larger design variable values towards the blade tip are caused by the presence of the autorotational inertia constraint which encourages the addition of mass at locations outboard. Figs. 6a and 6b depict the optimum versus the reference blade nonstructural segment weight distributions along the blade radius. For the rectangular blade (Fig. 6a) the optimum blade has lower nonstructural weight throughout the blade span. However, for the tapered blade (Fig. 6b) the optimum blade has larger nonstructural weight towards the blade tip than the reference blade. This is because the blade is tapered and has reduced structural weight at the blade tip and in order to satisfy the rotary inertia constraint, the nonstructural weight at the tip must increase.

Effect of Constraints on Higher Frequencies

This section of the paper investigates the effect of higher frequency constraints on the optimum blade weight and the optimum design variable distributions. Therefore, the results of the current work which involves constraints on five frequencies and rotary inertia (case b, Table 4) are compared with the results obtained by the authors in Ref. 19 with constraints on two frequencies and the rotary inertia (case c, Table 4). The results of this study are summarized in the last two columns of Tables 5 and 6 for rectangular blade (30 and 40 design variables, respectively) and Table 7 for tapered blade (42 design variables). Table 5 indicates that for the rectangular blade with 30 design variables, the optimum blade weight increases from 89.92 lbs in the two frequency case to 95.28 lbs in the five frequency case. However, the optimum blade with five frequency constraints is still 3 percent lighter than the reference blade. Tables 6 and 7 indicate similar trends for the rectangular blade with 40 design variables and the tapered blade with 42 design variables. There is also a change in the value of the taper ratio λ_h from 1.1 to 1.5 as shown in Table 7 suggesting that the blade taper increases with an increase in the number of frequency constraints. The optimization process raises the frequency f_1 (first lead-lag) to its prescribed upper bound and the autorotational inertia constraint is active in all the cases.

Figures 7-9 depict the design variable distributions (optimum versus reference) for the five and two frequency constraint cases. Fig. 7a depicts the horizontal box beam wall thickness (t_1) distributions along the blade span with 30 design variables for the rectangular blade. Fig. 7b depicts the same distribution for the tapered blade with 42 design variables. There are significant redistributions of the wall thicknesses between the five and two frequency constraint cases. For example, for the rectangular blade (Fig. 7a), in the five frequency constraint case (case b) the wall thickness (t_1) is smaller in magnitude at the blade root than the reference blade value but larger than the two frequency constraint case (case c). However, at the blade tip the value of t_1 in the five frequency constraint case is significantly smaller than its value in the two frequency constraint case, although both these values are larger than the reference blade value. The situation differs at the blade root in the tapered blade case (Fig. 7b) where the value of t_1 in the five frequency constraint case is smaller than the value for the two frequency constraint case. Figs. 8a and 8b present the box beam vertical wall thickness (t_2) distributions along the blade span for rectangular and tapered blades, respectively. The figures show that the value of t_2 in the five frequency constraint case is larger at the blade root than it is in the two frequency constraint case whereas the tendencies are reversed at the blade tip for both the rectangular and tapered blades.

Figs. 9a and 9b depict the nonstructural segment weight distributions along the blade span for the rectangular and the tapered blades, respectively. There is a significant reduction and change in the nonstructural weight distribution between the reference blade and the optimum blade in the two frequency constraint case than it is in the five frequency constraint case. In other words, the nonstructural weight distributions for the five frequency constraint case is closer to that of the reference blade. This is because the reference blade was designed with a larger number of design requirements on frequencies. There are significant differences in the optimum design variable distribution along the blade span between the two and five frequency constraint cases. This can be explained as follows. The mass and/or stiffness distribution tends to follow the pattern of the coupled mode shapes in the frequency constrained optimization. In the two frequency constraint cases, therefore, the mass distributions followed the mode shapes of the coupled first lead-lag dominated frequency and the first flapping dominated frequency. In the five frequency constraint cases, the mass distributions followed a different pattern as higher coupled frequencies are included.

Effect of Stress Constraints

The effect of adding centrifugal stress constraints to the optimum design with frequency and autorotational inertia constraints has also been investigated. The optimum designs with and without constraints on the stresses are compared in Tables 5-7. Table 5 indicates that for the rectangular blade with 30 design variables, the optimum blade weight increases with the addition of stress constraints. For example in Table 5, the blade weight reduction decreases from a value of 3.04 percent in case b to a value of 2.67 percent in case a. The differences in weight become more pronounced with an increase in the number of design variables (Tables 6 and 7). For the tapered blade there is very little change in the taper ratio. In all the cases studied, the optimization process still moves the first lead-lag frequency f_1 to its upper bound and the autorotational inertia constraint remains critical.

Some typical results showing the effect of stress constraints on optimum versus reference blade design variable distributions study are presented in Figs. 10-11. Figs. 10a and 10b depict the box beam horizontal wall thickness (t_1) distributions along the blade span with and without the stress constraints for both rectangular and tapered blades, respectively. The presence of stress constraints increases the wall thicknesses at the blade tip and reduces them inboard for the rectangular blade with 30 design variables (Fig. 10a). However, the tendencies are reversed in the tapered blade (Fig. 10b). Figs. 11a and 11b show the nonstructural weight distributions along the blade span for the rectangular and tapered blades, respectively. For the rectangular blade (Fig. 11a) the optimization process reduces the nonstructural weights at each segment (case b) and the inclusion of stress constraints (case a) only increases them a little. However for the tapered blade (Fig. 11b), the stress constraints increase the nonstructural segment weight at each segment making them higher than the reference blade values towards blade outboard.

Concluding Remarks

In this paper a procedure has been described for the minimum weight design of helicopter rotor blades with constraints on multiple coupled flap-lag natural frequencies, autorotational inertia and centrifugal stress. The design variables used are the box beam cross sectional dimensions, the magnitudes of the nonstructural segment weights and the blade taper ratio. The program CAMRAD has been used to calculate the mode shapes and frequencies of the blade and the program CONMIN has been used for the optimization. In addition, a linear approximation technique involving Taylor series expansion has been used to reduce analysis time. A sensitivity analysis consisting of analytical derivatives of the objective function, the autorotational inertia constraint and the stress constraints and a central finite difference scheme for the derivatives of the frequency constraints has been performed. Optimum designs have been obtained for blades with both rectangular and tapered planforms and compared with an existing (reference) blade. Studies have also been performed to assess the effects of higher frequency constraints and stress constraints on the optimum blade designs.

The following conclusions have been drawn from the present study. The optimization program CONMIN along with the linear approximations based on Taylor series expansions has been very efficient and optimum results have been obtained in typically eight to ten cycles. The results of the study indicate that there is an increase in the blade weight and a significant change in the design variable distributions with an increase in the number of frequency constraints. The optimization process tends to redistribute mass toward the blade tip due to the presence of the autorotational inertia constraint. The inclusion of the stress constraints has different effects on the wall thickness distributions of the rectangular and the tapered blades, but tends to increase the magnitude of the nonstructural segment weight distributions in both cases.

References

1. Ashley, H., "On Making Things the Best - Aeronautical Use of Optimization," AIAA J. Aircraft 19, No. 1, 1982.

2. Sobieszczanski-Sobieski, J., "Structural Optimization Challenges and Opportunities," presented at Int. Conference on Modern Vehicle Design Analysis, London, England, June 1983.

3. Miura, H., "Application of Numerical Optimization Method to Helicopter Design Problems: A Survey," NASA TM 86010, October 1984.

4. Bennett, R. L., "Application of Optimization Methods to Rotor Design Problems," Vertica, Vol. 7, No. 3, 1983, pp. 201-208.

5. Sobieszczanski-Sobieski, J., "Recent Experiences in Multidisciplinary Analysis and Optimization," NASA CP 2327, 1984.

6. Peters, D. A., Ko, Timothy, Rossow, Mark P., "Design of Helicopter Rotor Blades for Desired Placement of Natural Frequencies," Proc. of the 39th Annual Forum of the AHS, May 9-11, 1983, St. Louis, Missouri.

7. Venkayya, V. B. and Tischler, V. A., "Optimization of Structures with Frequency Constraints," Computer Methods for Nonlinear Solids and Structural Mechanics; Proc. of the Applied Mechanics, Bioengineering, and Fluids Engineering Conference, Houston, Texas, June 20-22, 1983.

8. Khot, N. S., "Optimization of Structures with Multiple Frequency Constraints," AFWAL-TI-83-29-FIBR-201, Wright-Patterson Air Force Base, Ohio, 1983.

9. Chattopadhyay, Aditi, Hanagud, S. V. and Smith, C. V., Jr., "Minimum Weight Design of a Structure with Dynamic Constraints and a Coupling of Bending and Torsion," Proc. of the 27th Structures, Structural Dynamics and Materials Conference, May 19-21, 1986, San Antonio, Texas.

10. Hanagud, S. V., Chattopadhyay, Aditi and Smith, C. V., Jr., "Optimum Design of a Vibrating Beam with Coupled Bending and Torsion," AIAA Journal, Vol. 25, No. 9, September 1987.

11. Reichert, G., "Helicopter Vibration Control - A Survey," Vertica, Vol. 5, 1981, pp. 1- 20.

12. Friedmann, P. P., "Response Studies of Rotors and Rotor Blades with Application to Aeroelastic Tailoring," Semi-Annual Progress Report on Grant NSG-1578, December 1981.

13. Taylor, R. B., "Helicopter Vibration Reduction by Rotor Blade Modal Shaping", Proc. of the 38th Annual Forum of the AHS, May 4-7, 1982, Anaheim, California.

14. Bennett, R. L., "Optimum Structural Design," Proc. of the 38th Annual Forum of the AHS, May 4-7, 1982, Anaheim, California, pp. 90-101.

15. Friedmann, P. P. and Shantakumaran, P., "Optimum Design of Rotor Blades for Vibration Reduction in Forward Flight," Proc. of the 39th Annual Forum of the AHS, May 9-11, 1983, St. Louis, Missouri.

16. Peters, D. A., "Design of Helicopter Rotor Blades for Optimum Dynamic Characteristics," Progress Report on Grant NAG-1-250, January 1985.

17. Hanagud, S., Chattopadhyay, Aditi, Yillikci, Y. K., Schrage, D., and Reichert, G., "Optimum Design of a Helicopter Rotor Blade," Paper No. 12, Proc. of the 12th European Rotorcraft Forum, September 22-25, 1986, Garmisch-Partenkirchen, West Germany.

18. Peters, D. A., Ko, Timothy, Korn, Alfred, and Rossow, Mark P., "Design of Helicopter Rotor Blades for Optimum Dynamic Characteristics," Progress Reports, NASA Research Grant Number NAG-1-250, January 1982 through January 1985.

19. Chattopadhyay, Aditi and Walsh, Joanne L., "Minimum Weight Design of Rectangular and Tapered Helicopter Rotor Blades with Frequency Constraints," Proc. of the 2nd Int. Conference on Rotorcraft Basic Research, February 16-18, 1988, College Park, Maryland. Also available as NASA TM 100561, February 1988.

20. Johnson, W., "A Comprehensive Analytical Model of Rotorcraft Aerodynamics and Dynamics," Part II: User's Manual, NASA TM 81183, June 1980.

21. Lang, K. W., and Nemat-Nasser, S., "An Approach for Estimating Vibration Characteristics of Nonuniform Rotor Blades," AIAA Journal, Vol. 17, No. 9, September 1979.

22. Johnson, W., "A Comprehensive Analytical Model of Rotorcraft Aerodynamics and Dynamics," Part I: Analysis Development, NASA TM 81182, June 1980.

23. Vanderplaats, G. N., "CONMIN - A Fortran Program for Constrained Function Minimization," User's Manual, NASA TMX-62282, August 1973.

Table 1. Reference blade data (Fig. 2)

Segment Number	Length (ft)	Box beam dimension (ft)			Bending stiffness x 10^4 (lb - ft^2)		Torsional stiffness x 10^4 (lb-ft^2)	Nonstructural segment weight (lbs) W_o		Pretwist (deg.)
	L	t_1	t_2	t_3	EI_x	EI_y	GJ	Total	Min.	
1	1.37	0.0116	0.0080	0.0280	7.349	78.58	11.111	6.718	0.89	1.745
2	2.2	0.0100	0.0100	0.0440	6.957	84.68	10.139	9.088	1.435	2.617
3	2.2	0.0075	0.0075	0.0325	5.548	66.55	7.778	1.978	1.435	5.594
4	2.2	0.0060	0.0050	0.0050	4.128	35.40	5.833	1.435	1.435	8.725
5	2.2	0.0050	0.0050	0.0045	3.537	31.20	5.000	2.352	1.435	6.805
6	2.2	0.0050	0.0050	0.0035	3.514	29.89	4.861	5.852	1.435	5.235
7	2.2	0.0050	0.0050	0.0040	3.526	30.55	4.931	6.342	1.435	3.49
8	2.2	0.0050	0.0050	0.0046	3.539	31.31	5.000	6.573	1.435	0.00
9	2.2	0.0050	0.0050	0.0035	3.514	29.89	4.861	6.372	1.435	-0.175
10	2.2	0.0050	0.0050	0.0021	3.481	27.91	2.778	5.962	1.435	-1.915

Table 2. Blade preassigned properties

Number of blades	4
Blade radius	22 ft.
Chord	1.3 ft.
Flap hinge offset	0.833 ft.
Inplane hinge offset	0.833 ft.
Solidity (based on mean chord)	0.0748
Precone angle	0 degree
Droop angle	0 degree
Tip sweep	0 degree
Pitch axis droop	0 degree
Pitch axis sweep	0 degree
Rotor speed	293 rpm

Table 3. Reference blade frequencies and bounds (windows)

	Reference Blade Frequency		Prescribed Bounds			
			lower		upper	
	Hz	per rev	Hz	per rev	Hz	per rev
f_1	12.285	2.52	12.162	2.49	12.408	2.54
f_2	16.098	3.30	15.936	3.26	16.258	3.33
f_3	20.913	4.28	20.704	4.24	21.122	4.33
f_4	34.624	7.09	34.272	7.02	34.966	7.16
f_5	35.861	7.34	35.502	7.27	36.219	7.42

Table 4. Summary of cases studied

Constraint Case	No. of Design Variables	Planform	Design variables (i=1,2,...,10)
a	30	Rectangular	$t_{1_i}, t_{2_i}, t_{3_i}$
b	30	Rectangular	$t_{1_i}, t_{2_i}, t_{3_i}$
c	30	Rectangular	$t_{1_i}, t_{2_i}, t_{3_i}$
a	40	Rectangular	$t_{1_i}, t_{2_i}, t_{3_i}, W_{o_i}$
b	40	Rectangular	$t_{1_i}, t_{2_i}, t_{3_i}, W_{o_i}$
c	40	Rectangular	$t_{1_i}, t_{2_i}, t_{3_i}, W_{o_i}$
a	42	Tapered	$h_r, \lambda_h, t_{1_i}, t_{2_i}, t_{3_i}, W_{o_i}$
b	42	Tapered	$h_r, \lambda_h, t_{1_i}, t_{2_i}, t_{3_i}, W_{o_i}$
c	42	Tapered	$h_r, \lambda_h, t_{1_i}, t_{2_i}, t_{3_i}, W_{o_i}$

Case	Constraint definition	Abbreviation used
a	Windows on first three lead-lag and first two flapping frequencies, autorotaional inertia and stress constraints	5 freq,AI,σ
b	Windows on first three lead-lag and first two flapping frequencies and autorotational inertia constraint	5 freq,AI
c	Windows on first lead-lag and first flapping freq. and autorotational inertia constraint (Ref. 19)	2 freq,AI

Table 5. Optimization results for rectangular blade; cases a-c, 30 design variables (see Table 4)

	Reference blade	Optimum blade		
		5 Freq AI σ case a	5 Freq AI - case b	2 Freq AI - case c
f_1 (Hz)	12.285	12.408	12.408	12.408
f_2 (Hz)	16.098	16.056	16.044	15.945
f_3 (Hz)	20.913	20.968	21.027	20.877
f_4 (Hz)	34.624	34.546	34.594	33.363
f_5 (Hz)	35.861	35.502	35.502	34.201
Autorotational inertia (lb-ft^2)	517.3	517.3	517.3	517.3
Blade weight (lb)	98.27	95.62	95.28	89.92
Percent reduction in blade weight*	-	2.67	3.04	8.50

* - From reference blade

Table 6. Optimization results for rectangular blade; cases a-c, 40 design variables (see Table 4)

	Reference blade	Optimum blade		
		5 Freq AI σ case a	5 Freq AI - case b	2 Freq AI - case c
f_1 (Hz)	12.285	12.408	12.408	12.408
f_2 (Hz)	16.098	16.075	16.025	15.940
f_3 (Hz)	20.913	21.081	21.060	22.600
f_4 (Hz)	34.624	34.823	34.689	37.050
f_5 (Hz)	35.861	35.800	35.595	38.710
Autorotational inertia (lb-ft^2)	517.3	517.3	517.3	517.3
Blade weight (lb)	98.27	93.613	90.624	85.270
Percent reduction in blade weight*	-	4.74	7.78	13.23

* - From reference blade

Table 7. Optimization results for tapered blade; cases a-c, 42 design variables (see Table 4)

	Reference blade	Optimum blade		
		5 Freq AI - σ case a	5 Freq AI - case b	2 Freq AI - case c
λ_h	1.0	1.490	1.508	1.111
f_1 (Hz)	12.285	12.408	12.408	12.408
f_2 (Hz)	16.098	16.066	16.064	15.938
f_3 (Hz)	20.913	20.888	20.959	22.504
f_4 (Hz)	34.624	34.678	34.646	36.753
f_5 (Hz)	35.861	35.507	35.525	38.447
Auto-rotational inertia (lb-ft^2)	517.3	517.3	517.3	517.3
Blade weight (lb)	98.27	92.16	89.24	84.24
Percent reduction in blade weight*	-	6.21	9.19	14.28

* - From reference blade

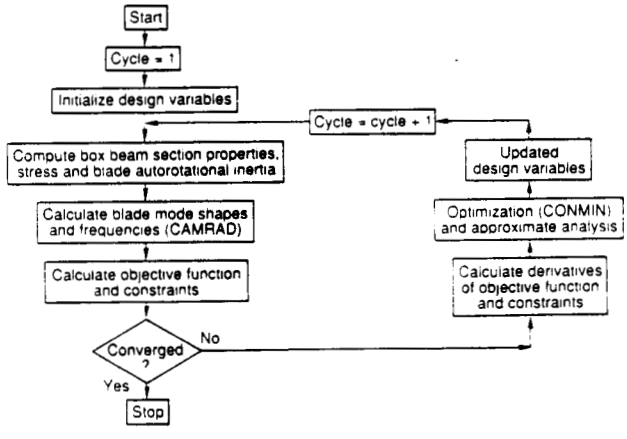

Fig. 1 Flowchart of the optimization process

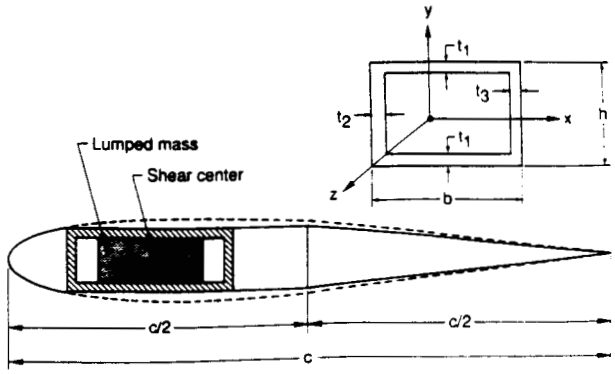

Fig. 2 Rotor blade cross section

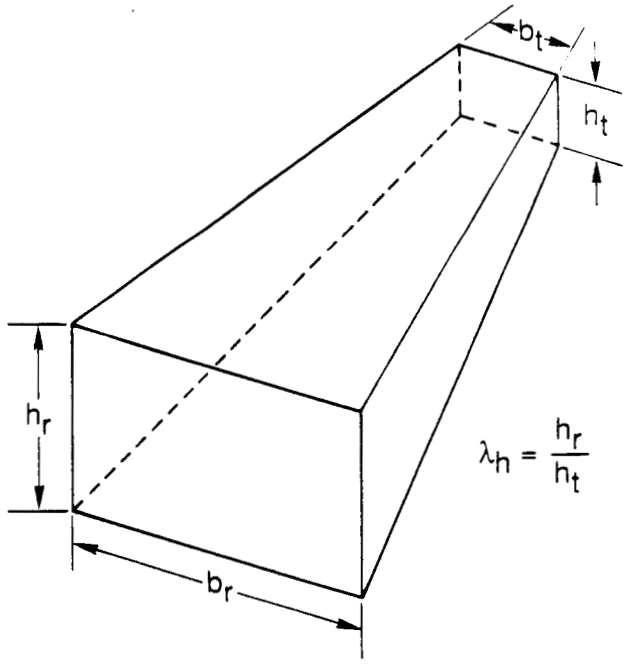

a) Tapered box beam

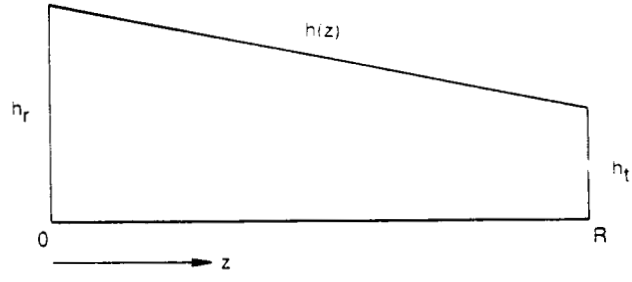

$h(z) = h_r(1-z/R) + h_t z/R$

b) Rotor blade taper

Fig. 3 Rotor blade

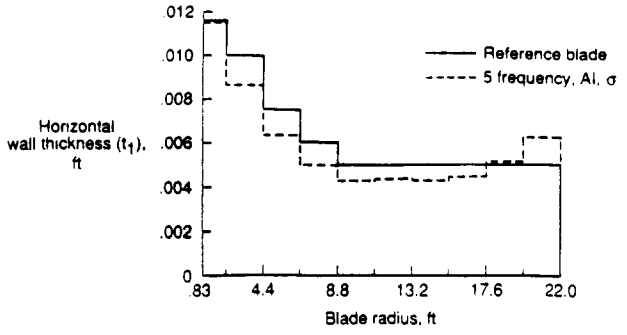

a) Rectangular blade, 30 design variables

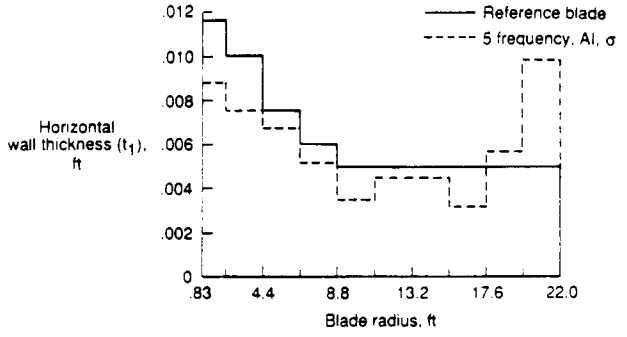

b) Tapered blade, 42 design variables

Fig. 4 Optimum distribution of box beam horizontal wall thickness (t_1) along blade radius

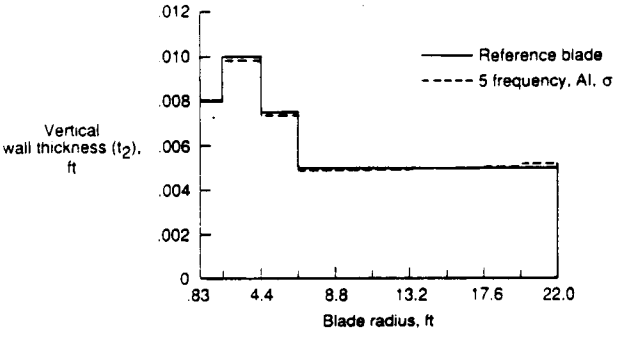

a) Rectangular blade, 30 design variables

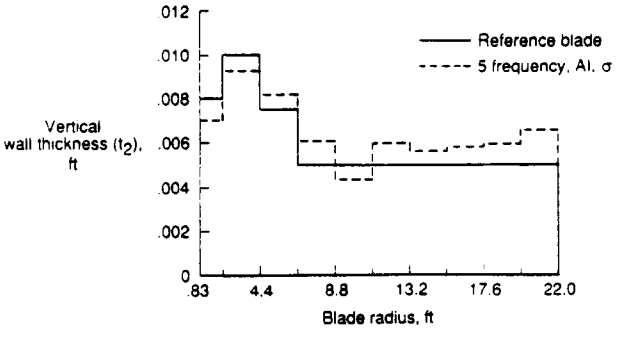

b) Tapered blade, 42 design variables

Fig. 5 Optimum distribution of box beam vertical wall thickness (t_2) along blade radius

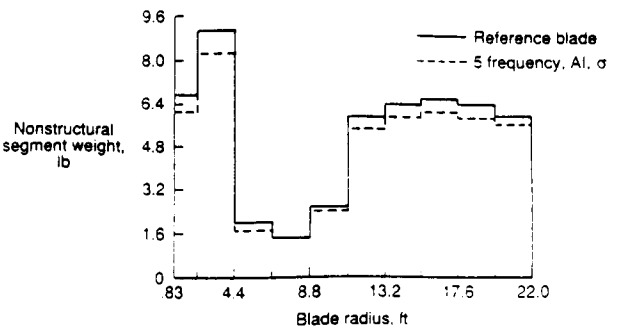

a) Rectangular blade, 40 design variables

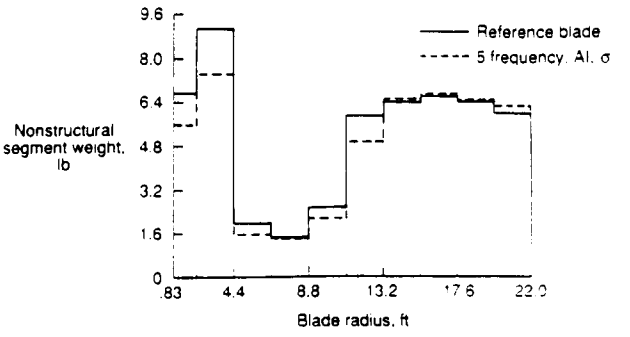

b) Tapered blade, 42 design variables

Fig. 6 Optimum distribution of nonstructural segment weight along blade radius

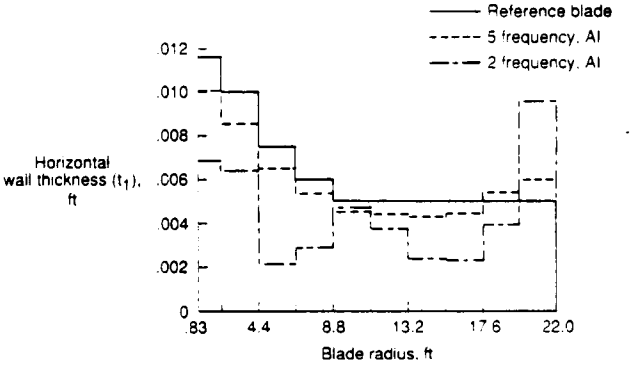

a) Rectangular blade, 30 design variables

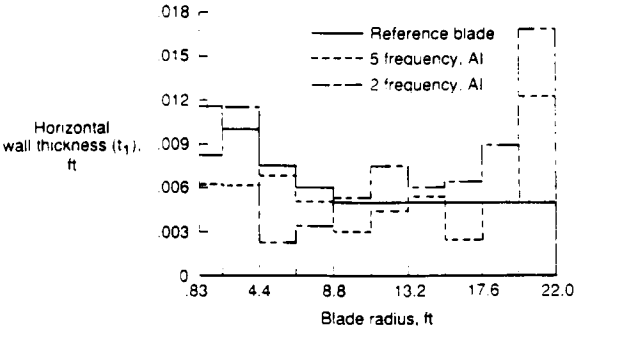

b) Tapered blade, 42 design variables

Fig. 7 Optimum distributions of box beam horizontal wall thickness (t_1) along blade radius; effect of higher frequency constraints

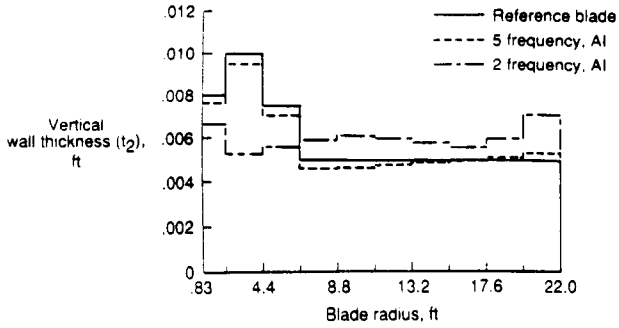

a) Rectangular blade, 30 design variables

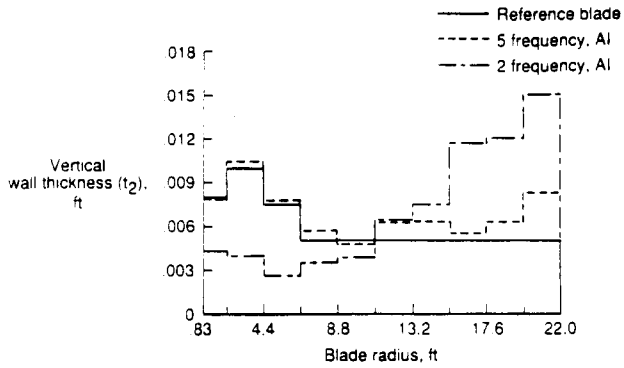

b) Tapered blade, 42 design variables

Fig. 8 Optimum distributions of box beam vertical wall thickness (t_2) along blade radius; effect of higher frequency constraints

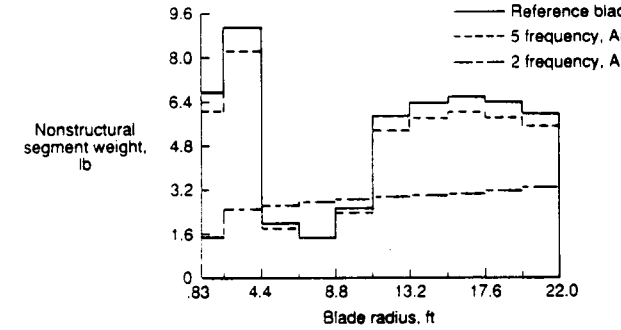

a) Rectangular blade, 40 design variables

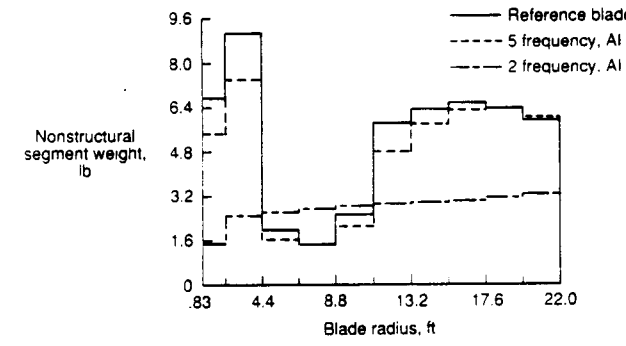

b) Tapered blade, 42 design variables

Fig. 9 Optimum distributions of nonstructural segment weight along blade radius

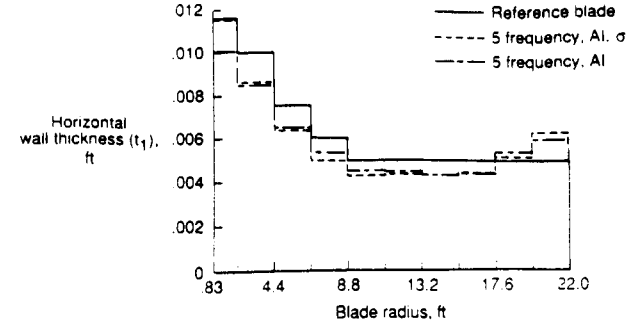

a) Rectangular blade, 30 design variables

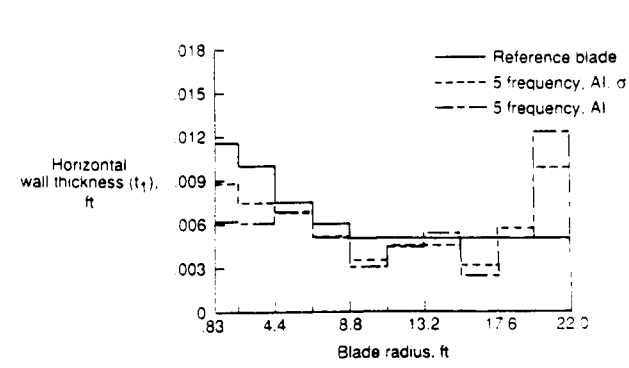

b) Tapered blade, 42 design variables

Fig. 10 Optimum distributions of box beam horizontal wall thickness (t_1) along blade radius; effect of stress constraints

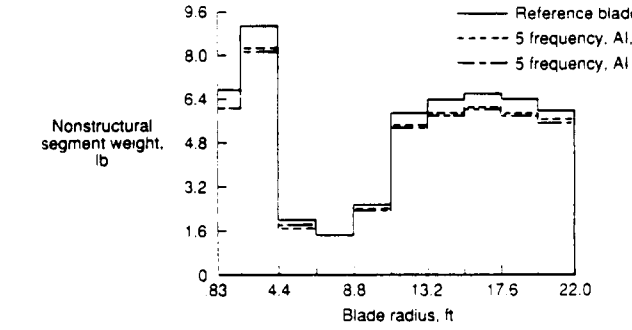

a) Rectangular blade, 40 design variables

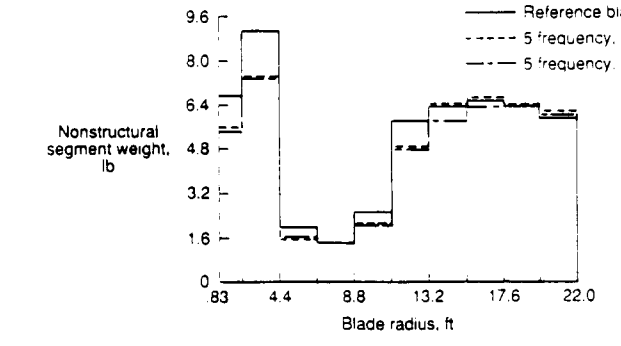

b) Tapered blade, 42 design variables

Fig. 11 Optimum distribution of nonstructural segment weight along blade radius; effect of stress constraints

NASA
National Aeronautics and Space Administration

Report Documentation Page

1. Report No.	2. Government Accession No.	3. Recipient's Catalog No.
NASA TM-100569		

4. Title and Subtitle

Minimum Weight Design of Rotorcraft Blades with Multiple Frequency and Stress Constraints

5. Report Date

March 1988

6. Performing Organization Code

7. Author(s)

Aditi Chattopadhyay
Joanne L. Walsh

8. Performing Organization Report No.

10. Work Unit No.

505-63-51-10

9. Performing Organization Name and Address

NASA Langley Research Center
Hampton, VA 23665-5225

11. Contract or Grant No.

13. Type of Report and Period Covered

Technical Memorandum

12. Sponsoring Agency Name and Address

National Aeronautics and Space Administration
Washington, DC 20546-0001

14. Sponsoring Agency Code

15. Supplementary Notes

Aditi Chattopadhyay, Analytical Services and Materials, Inc., Hampton, Virginia.
Joanne L. Walsh, Langley Research Center, Hampton, Virginia.
Presented at AIAA/ASME/ASCE/AHS 29th Structures, Structural Dynamics and Materials Conference, Williamsburg, VA, April 18-20, 1988.

16. Abstract Minimum weight designs of helicopter rotor blades with constraints on multiple coupled flap-lag natural frequencies are studied. Constraints are imposed on the minimum value of the blade autorotational inertia to ensure sufficient rotary inertia to autorotate in case of engine failure and on stresses to guard against structural failure due to blade centrifugal forces. Design variables include blade taper ratio, dimensions of the box beam located inside the airfoil and magnitudes of nonstructural weights. The program CAMRAD is used for the blade modal analysis; the program CONMIN is used for the optimization. A linear approximation involving Taylor series expansion is used to reduce the analysis effort. The procedure contains a sensitivity analysis consisting of analytical derivatives for objective function and constraints on autorotational inertia and stresses. Central finite difference derivatives are used for frequency constraints. Optimum designs are obtained for both rectangular and tapered blades. Using the method developed in this paper, it is possible to design a rotor blade with reduced weight, when compared to a baseline blade, while satisfying all the imposed design requirements. The effect of adding higher frequency and stress constraints on optimum blade weight and optimum mass and stiffness distributions is also discussed.

17. Key Words (Suggested by Author(s))

Helicopter
Dynamics
Rotor blade
Optimization
Stress
Frequency
Minimum Weight
Autorotational

18. Distribution Statement

Unclassified - Unlimited
Star Category 05

19. Security Classif. (of this report)	20. Security Classif. (of this page)	21. No. of pages	22. Price
Unclassified	Unclassified	13	A02